A New Look at the Classical Beckmann Rearrangement: A Strong Case of Active Solvent Effect

ARTICLE *in* JOURNAL OF THE AMERICAN CHEMICAL SOCIETY · MARCH 1997

Impact Factor: 12.11 · DOI: 10.1021/ja962364q

3 AUTHORS, INCLUDING:

Minh Tho Nguyen
University of Leuven
748 PUBLICATIONS **10,835** CITATIONS
SEE PROFILE

L. G. Vanquickenborne
University of Leuven
174 PUBLICATIONS **3,357** CITATIONS
SEE PROFILE

A New Look at the Classical Beckmann Rearrangement: A Strong Case of Active Solvent Effect

Minh Tho Nguyen,* Greet Raspoet, and Luc G. Vanquickenborne

Contribution from the Department of Chemistry, University of Leuven, Celestijnenlaan 200F, B-3001 Leuven, Belgium

Received July 10, 1996. Revised Manuscript Received October 21, 1996[⊗]

Abstract: Substituent and solvent effects on the reaction pathway of the Beckmann rearrangement were studied. Energy surfaces of the isolated gas phase systems were mapped out using ab initio MO calculations at the MPn and QCISD(T) levels with basis sets ranging from 6-31G(d,p) to 6-311++G(2df,2p). In the simplest gas phase system, the most favored path is as follows: protonation of formaldehyde oxime → N-protonated species → O-protonated species → fragmentation products, in which the 1,2-H-shift connecting both protonated isomers is rate-determining. While both methyl and formyl substituents on C and O of the oxime have only a small effect on the rate-controlling energy barrier, they significantly modify the barrier to fragmentation. The bulk solvent effect which is treated by a polarizable continuum model does affect only marginally the activation parameters with respect to the gas phase values. A combination of both quantum and statistical mechanics was also used to probe the solvent effect. In order to investigate the active role of the solvent, ab initio calculations were carried out within a supermolecule approach. An active participation of one solvent molecule in a reacting supersystem gives rise to a genuine effect. As simple solvent molecules, H_2O, $H_2C{=}O$, and HCOOH were studied, the latter being a model for the Beckmann solution (HCl + acetic acid + acetic anhydride). While their involvement as a coreactant considerably reduces the barrier of the 1,2-H-shift by about 50% and hence approaches the experimental results, the effect of the bulk solvent on the reacting supersystem remains small. The calculated results suggest that the Beckmann rearrangement represents a strong case of active solvent participation, which consists in assisting the rate-determining 1,2-H-shift by catching the migrating hydrogen of the substrate and putting it back at the other end; the migration is thereby considerably accelerated.

Introduction

More than a century ago, Beckmann[1] first carried out in 1886 the conversion of an oxime (I) into an amide (IV) (eq 1); since then, this reaction has been called after his name, the Beckmann rearrangement.

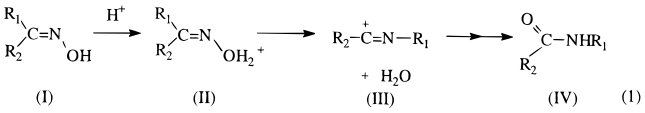

With the test of time the Beckmann rearrangement (designated hereafter as BR) has proven to constitute one of the most widely employed transformations of oximes in organic synthesis. The conversion of cyclohexanone oxime into ϵ-caprolactam which is a basic component for the fabrication of Nylon 6 has been a textbook example[2] for years. As one of the classical and most popular reactions in organic chemistry, it has been indeed reviewed several times.[3−14] As far as the BR mechanism is concerned, it is commonly assumed that the reaction involves an initial protonation at oxygen of an oxime (I) giving an oxonium cation (II) and followed by a migration of an alkyl group (R_1) plus a departure of a water molecule giving a nitrilium cation (III). The latter ion is in turn hydrolyzed in basic solution yielding finally an amide (IV). In spite of the wealth of results[3−14] that have been reported during the last century on the synthetic and industrial applications of the BR of oximes, the mechanistic aspects of this reaction remain poorly understood. Although the rate constants and the associated activation energies of the BR could be measured in many cases,[15,16] the nature of its rate-determining step has not been identified experimentally yet. For the purpose of interpretation, the migration plus elimination step (II) → (III), characterized by a migration from C to N of the substituent R_1 having an anti conformation relative to the departing hydroxyl group, has often been assumed to be rate-determining, even though there has been neither kinetic nor spectroscopic supporting evidence.

Experiments[15] have shown that an increase in the dielectric constant of the reaction medium appears to augment the rate of the rearrangement. Moreover, solvents of high nucleophilic power, such as water, amines, or alcohols also increase the rearrangement rate. Nevertheless, the latter solvents cannot be used in practice. The most common media for BR are concentrated sulfuric acid (oleum), phosphorus pentachloride in ether, and a Beckmann solution; the latter consists of

[⊗] Abstract published in *Advance ACS Abstracts,* March 1, 1997.

(1) Beckmann, *E. Chem. Ber*. **1886**, *89*, 988.
(2) Hendrickson, J. B; Cram, D. J.; Hammond, G. S. *Organic Chemistry*, 3d ed.; McGraw-Hill: Tokyo, 1970; p 708.
(3) Blatt, A. H. *Chem. Rev.* **1933**, *12*, 215.
(4) Jones, B. *Chem. Rev.* **1944**, *35*, 335.
(5) Moller, F. in *Methoden der Organischen Chemie*; Muller, E., Ed., Thieme Verlag: Stuttgart, 1957; Vol. 11, Part 1, p 892.
(6) Donaruma, L. G.; Heldt,W. Z. *Org. React.* **1960**, *1*, 11.
(7) Beckwith, A. L. J. In *The Chemistry of Amides*; Zabicky, J., Ed.; Interscience: New York, 1970; p 131.
(8) McCarty, C. G. In *The Chemistry of the Carbon Nitrogen Double Bond*; Patai, S., Ed.; Interscience: New York, 1970; p 408.
(9) Smith, P. A. S. In *Molecular Rearrangements*; De Mayo, P., Ed.; Interscience: New York, 1963; p 45.
(10) Mukamal, H. *Nuova Chim*. **1971**, *47*, 79.
(11) Hornke, G.; Krauch, H.; Kunz, W. *Chem.-Zgt.* **1965**, *89*, 525.
(12) Gawley, R. E. *Org. React*. **1988**, *35*, 1.
(13) Jochims, J. C.; Hehl, S.; Herzberger, S. *Synthesis* **1990**, 1128.
(14) Hesse, M. *Ring Enlargement in Organic Chemistry*, VCH: Weinheim, 1991.
(15) Heldt, W. Z. *J. Org. Chem*. **1961**, *26*, 1695.
(16) Zarakhani, N. G. *Russ. Chem. Rev.* **1967**, *36*, 51.

S0002-7863(96)02364-5 CCC: $14.00

concentrated hydrogen chloride in a mixture of acetic acid and acetic anhydride. The kinetics of the rearrangement of different oximes in acetic acid were measured spectrophometrically,[15] and the corresponding activation barriers were determined to be about 80−100 kJ·mol^{-1}. If a high yield of amide is desired, added fuming sulfuric acid has been recommended which prevents secondary reactions such as hydrolysis. We would like to mention in particular a review on the kinetics of the BR of alicyclic oximes under the action of oleum and Beckmann's mixture written by Vinnik and Zarakhari[16] in 1967.

Recent theoretical studies[17−18] showed that the N-protonation of formaldehyde oxime is largely preferred over the O-protonation. In the simplest model case, the N-protonated form differs by about 70−80 kJ·mol^{-1} from the O-protonated form, in favor of the former. Calculated results also suggest that, following the formation of the N-protonated oxime, a direct 1,2-hydrogen shift constitutes the easiest pathway producing its O-protonated isomer. In gas phase, the energetically most favored route is given in eq 2: N-protonation of formaldehyde oxime → O-protonated oxime → BR products.

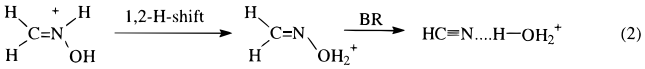

(2)

In this regard, the O-protonated oxime appears to be an indispensible intermediate of the BR, whose formation via a 1,2-H-shift is much more difficult to achieve than its transformation. The energy barriers are calculated to be 225 and 44 kJ·mol^{-1}, respectively, at the MP4/6-311++G(d,p) + ZPE level of MO theory; formation of the O-protonated oxime is clearly the rate-determining step for the gas phase process. It should be stressed that although the N-protonation is preferred in gas phase, a certain population of O-protonated forms is expected to exist, since protonation occurs without any barrier. Nevertheless, in view of the large difference in energy between both forms mentioned above, the equilibrium should be strongly displaced toward the N-protonated species. It is therefore reasonable to assume that the key step in the gas phase BR is actually the 1,2-H-shift connecting the N- to the O-protonated form.

While the calculated barrier to 1,2-H-shift is about twice as large as the experimental values of about 100 kJ·mol^{-1} measured in different solvents, as mentioned above,[15,16] the calculated barrier to rearrangement is relatively too small. The large difference between the theoretical activation energy for model systems and experimental values indicates the crucial role of the substituents and/or the solvent in accelerating the 1,2-H-shift. In the present work, we make a new attempt to understand this intriguing problem and report here a computational study on both substituent and solvent influences. To simulate the substituent effect, methyl substitution at both carbon and oxygen centers as well as the oxime ether with a formyl group at oxygen has been considered. Regarding the solvent, both passive and active aspects of its effect have been investigated using both continuum and supermolecule approaches as well as a combination of both quantum and statistical mechanics treatments. Overall, calculated results provide fundamental novel insights into the BR mechanism which actually challenge the prevailing perceptions. It is suggested that the solvent plays an active role as a catalyst during a BR transformation of an oxime.

(17) Nguyen, M. T.; Vanquickenborne, L. G. *J. Chem. Soc., Perkin Trans.* 2 **1993**, 1969.

(18) Nguyen, M. T.; Raspoet G., Vanquickenborne, L. G. *J. Chem. Soc., Perkin Trans. 2* **1995**, 1791.

Methods of Calculation

Ab initio molecular orbital calculations were carried out using a local version of the GAUSSIAN 92[19] set of programs. The stationary points of interest were initially located and characterized by harmonic vibrational analysis employing energy hessians at the Hartree−Fock (HF) with the dp-polarized 6-31G(d,p) basis set. The relevant structures were then reoptimized at second-order Møller−Plesset Perturbation Theory (MP2) level with the same basis set, using both HF geometries and hessians as starting points. The identity of the stationary points were, however, not characterized again by vibrational analysis at the MP2 level, simply due to the high CPU cost in computing MP2 hessians. Due to the fact that for most of the points considered, both HF and MP2 geometrical parameters do not differ from each other, we are confident that their identity can be safely established by the HF hessians. Improved relative energies between stationary points were finally estimated using full fourth-order perturbation (MP4SDTQ) and quadratic configuration interaction (QCISD(T)) methods and both the larger 6-311G(d,p) and the sp-diffuse plus dp-polarized 6-311++G-(d,p) basis sets at MP2/6-31G(d,p) optimized geometries. These values were further corrected for zero-point vibrational energies (ZPE).

The understanding of the effect of solvation on reaction rates has been tackled employing different approaches. In the first, the solvent molecules are considered explicitly, and quantum chemical calculations are performed for a solute and a few interacting solvent molecules, called a reacting supermolecule. Three simple models of solvent molecules were studied including water (H_2O), used as a reference, formic acid (HCOOH), the closest model for a reaction process in a "Beckmann mixture" (HCl plus acetic acid plus acetic anhydride), and finally formaldehyde (H_2CO), used to check the influence of the hydroxyl group in acetic acid. In this approach which considers an active participation of the solvent molecule, the stationary structures of interest were computed at the same level as the gas phase results. An alternative approach is to model the solvent as a dielectric continuum. In this passive model, the solvent is placed in a cavity immersed in a continuous medium, characterized by its dielectric constant ϵ. The electronic distribution of the solute polarizes the continuum and generates an electric field inside the cavity which in turn affects the solute's geometry and electronic structure. For this purpose, we employed two distinct models including the classical Onsager self-consistent reaction field (SCRF)[20] and the more advanced polarizable continuum model (PCM).[21] Implementation of the PCM interaction scheme was developed by Tomasi and coworkers.[21] Finally, a combined model, as worked out by Van Duijnen et al.,[22] was also used to probe further the solvent effect. Details of the calculations will be given in the related sections. In the following discussion, the term BR refers to the entire process, even though it is originally employed to describe the migration-elimination step of an O-protonated oxime. Throughout this paper, bond lengths are given in Å, bond angles in

(19) Frisch, M. J.; Trucks, G. W; Head-Gordon, M.; Gill, P. M. W.; Wong, M. W.; Foresman, J. G.; Johnson, B. G.; Schlegel, H. B.; Robb, M. A.; Replogle, E. S.; Comperts, R.; Andres, J. L.; Fox, D. J.; Defrees, D. J; Baker, J.; Stewart, J. J. P.; Pople, J. A. Gaussian 92; Gaussian Inc.: Pittsburgh, PA, 1992.

(20) Wong, M. W., Frisch, M. J.; Wiberg, K. B. *J. Am. Chem. Soc.* **1991**, *113*, 4776.

(21) Miertus, S.; Scrocco, E.; Tomasi, J. *Chem. Phys.* **1981**, *55*, 117.

(22) (a) Depuis, M.; Maluendes, S. A. In *Modern Techniques in Computational Chemistry*; Clementi, E., Ed.; ESCOM: Leiden, 1991; Chapter 8. (b) Van Duijnen, P. Th.; Juffer, A.H.; Dijkman, J. P. *J. Mol. Struct. (Theochem)* **1992**, *260*, 195. (c) De Vries, A. H.;Van Duijnen, P. Th.; Juffer, A. H. *Int. J. Quant. Chem. Symp.* **1993**, *27*, 451.

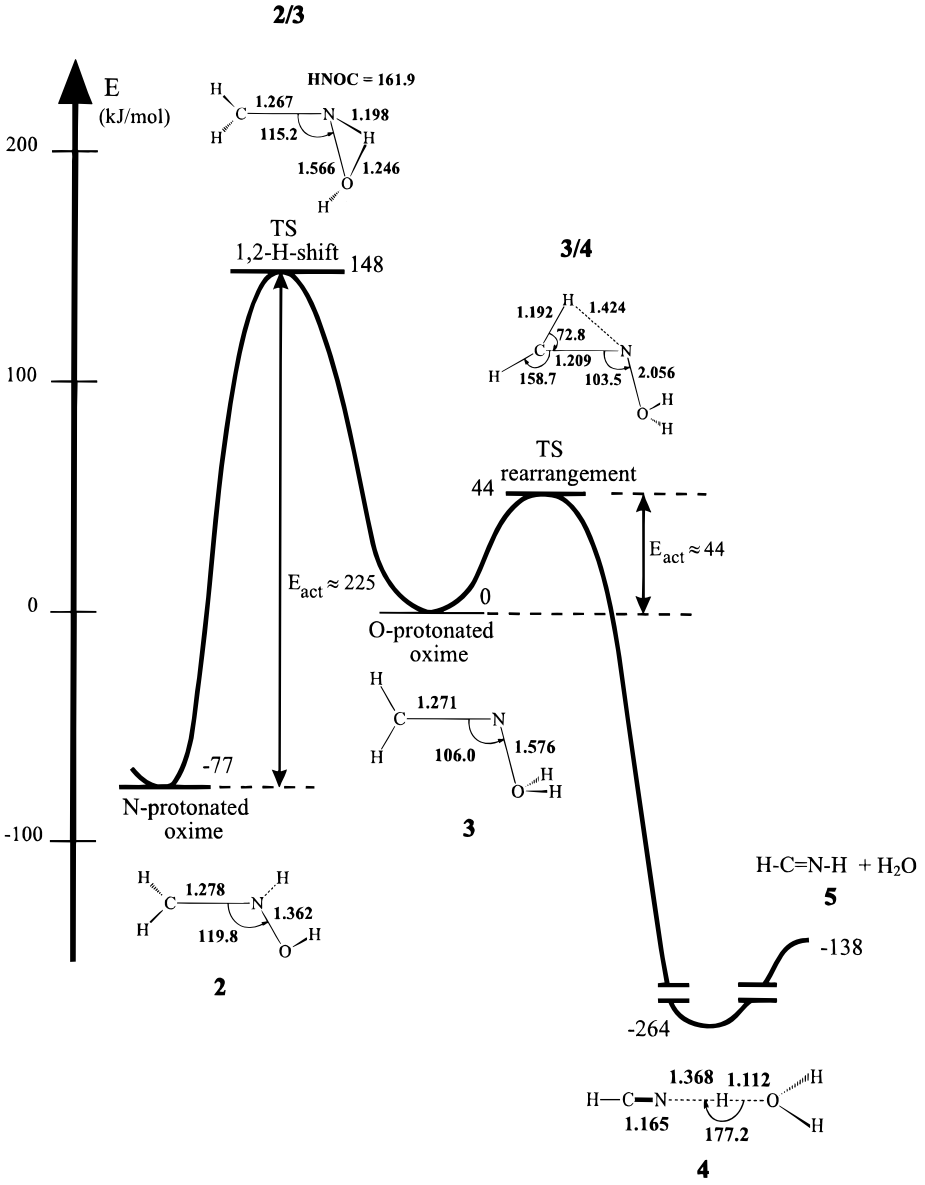

Figure 1. Schematic energy profile showing the Beckmann process of protonated formaldehyde oxime in the gas phase. All structures considered are charged +1. Values at MP4/6-311++G(d,p) + ZPE level, based on MP2/6-31G(d,p) optimized geometries.

degrees, zero-point vibrational (ZPE) and relative energies, unless otherwise stated, in kJ·mol^{-1}. All total energies in hartrees are available as Supporting Information (four tables).

Results and Discussion

The Unsubstituted Gas Phase System $(CH_4NO)^+$. Before examining the substituent and solvent effects, it is useful to recall the essential results for the unsubstituted gas phase system. In a recent paper[18] we have reported a detailed exploration of the $[CH_4NO]^+$ potential energy surface related to the gas phase BR, whose essential features are summarized in Figure 1. A predominant N-protonation of formaldehyde oxime gives rise to a N-protonated oxime **2** which should be first converted to its O-protonated isomer **3**. Then a migration-elimination could take place from **3** giving the nitrilium ion complex **4**. In ref 18, the potential energy surface has been mapped out by making use of perturbation theory MP4SDTQ/6-311++G(d,p) + ZPE calculations based on MP2/6-31G(d,p) optimized geometries. In order to assess further the dependency of the thermochemical quantities with respect to the computational methods, we have carried out a series of calculations on these structures using different atomic functions and methods (see Table 1). The quadratic configuration interaction method represents an improved treatment of electron correlation, relative to the MPn method, and consists therefore in testing the convergence behavior of the MPn perturbative expansions. These calculations also serve as a calibration for larger systems for which only MP4 calculations could be performed. From the results listed in Table 1, a few points could be noted.

(i) Relative energies obtained by MP4SDTQ, QCISD, and QCISD(T) calculations are rather similar, the differences lying within the expected error bars. This indicates that the energies of the structures under consideration can reasonably be calculated by using MPn expansions.

(ii) Except for the fragmentation products **5**, the MP4-values obtained with both 6-311G(d,p) and 6-311++G(d,p) basis sets are fairly close to each other. The larger deviation for **5** reflects the difficulty in computing the proton affinity of HCN, and,

(iii) Extension of atomic basis tends to enlarge the energy difference **2** and **3** in favor of **2** and thereby lowers the energy of the TS for 1,2-H-shift **2/3** relative to **3**. However, it is beyond doubt that the 1,2-H-shift is the rate-controlling step. Overall, the systematic comparison in Table 1 indicates that the

Table 1. Comparison of Relative Energies along the BR of Protonated Formaldoxime Obtained by Different MO methods[a]

method	geometry[b]	**2**	**2/3**	**3**	**3/4**	**4**	**5**
MP2/6-31G(d)	MP2/6-31G(d)	−55	146	0	68	−257	−120
MP2/6-31G(d,p)	MP2/6-31G(d,p)	−83	141	0	59	−277	−126
MP2/6-311G(d,p)		−78	142	0	47	−284	−141
MP2/6-311++G(d,p)		−84	142	0	42	−290	−160
MP2/6-311++G(2df,2p)		−92	135	0	50	−282	−157
MP4/6-311G(d,p)	MP2/6-31G(d)	−69	147	0	49	−260	−121
MP4/6-311++G(d,p)	MP2/6-31G(d,p)	−77	148	0	44	−264	−138
QCISD/6-311++G(d,p)		−82	161	0	49	−255	−130
QCISD(T)/6-311++G(d,p)		−77	152	0	48	−254	−135

[a] Relative energies include ZPE corrections. Core orbitals are frozen in correlation treatments. [b] MP2/6-31G(d,p) optimized geometries taken from ref 18 are not much different from the MP2/6-31G(d) geometries. See Figure 1 for definition of the structures.

Table 2. Geometrical Parameters Related to the C=N−O Skeleton upon Methyl Substitution at C and O of Oximes

species[a]		*r*(C=N)	*r*(N−O)	CNO
oxime	**1**	1.284	1.411	110.0
	1Z	1.285	1.416	109.8
	1E	1.286	1.417	110.0
	1D	1.291	1.421	110.1
	1M	1.284	1.405	110.0
	1F	1.281	1.425	109.0
NH^+-oxime	**2**	1.280	1.366	119.8
	2Z	1.288	1.372	121.1
	2E	1.285	1.374	120.2
	2D	1.295	1.377	120.9
	2M	1.280	1.354	120.9
	2F	1.280	1.370	120.6
OH^+-oxime	**3**	1.271	1.577	106.0
	3Z	1.274	1.596	108.0
	3E	1.276	1.582	106.2
	3D	1.278	1.605	107.6
	3M	1.275	1.541	106.6
	3F	1.276	1.529	106.9

[a] Values at the MP2/6-31G(d) level. **Z** stands for *Z*-$(CH_3)HC{=}NOH$; E for *E*-$(CH_3)HC{=}NOH$; **D** for $(CH_3)_2HC{=}NOH$; **M** for $H_2C{=}N$-OCH_3; and **F** for $H_2C{=}N{-}O{-}CH{=}O$.

Table 3. Calculated Proton Affinities of *C*-Methyl Oximes[a]

oxime	notation	PA(N)	PA(O)	ΔPA[c]
$H_2C{=}N{-}OH$		812 (792)[b]	743	69
Z-$(H_3C)HC{=}N{-}OH$	**Z**	851	763	88
E-$(H_3C)HC{=}N{-}OH$	**E**	850	773	77
$(CH_3)_2C{=}N{-}OH$	**D**	1092	1001	91
$H_2C{=}N{-}OCH_3$	**M**	836	776	60
H2C=N−O−CH=O	**F**	802	740	62

[a] Based on MP4/6-311G(d,p)//MP2/6-31G(d) + ZPE calculations in kJ·mol^{-1}. [b] The best estimate from heats of formation, see ref 18. [c] ΔPA = PA(N) − PA (O).

MP4SDTQ/6-311G(d,p)//MP2/6-31G(d) level can be employed for larger substituted systems.

Substituent Effects. Turning now to the effect of substituents on the basic features of the BR, we have considered methyl substitution at carbon and substitution at oxygen by both methyl and formyl groups. Calculated results are summarized in Table 2−4 and illustrated in Figures 2−4.

(a) The Methyl and Dimethyl C-Substituted Species. The purpose of examining both *Z*- and *E*-$(CH_3)HC{=}$N-OH and $(CH_3)_2C{=}$N-OH systems is 3-fold: (1) the *Z*-$(CH_3)HC{=}NOH$ species models the effect of a C-alkyl group on hydrogen migration; (2) the *E*-$(CH_3)HC{=}$N-OH species allows the migratory aptitude of an alkyl group to be evaluated, and (3) the $(CH_3)_2C{=}$N-OH species provides a better model for larger oximes such as cyclohexanone oxime.

As mentioned above, for these systems only electronic energy calculations at the MP4SDTQ/6-311G(d,p) level employing MP2/6-31G(d)-optimized geometries were carried out. Characterization of the stationary points and evaluation of the ZPEs were based on HF/6-31G(d)-wave functions. The structure of formaldehyde oxime has been the subject of a number of previous studies[17,18] and thus warrants no further comment. For each system, we have considered both N-protonated **2** and O-protonated **3** species, the product complex **4**, the product fragments **5**, the transition structure for 1,2-H-shift **2/3**, and the transition structure for migration-elimination **3/4** (see Figure 1). Because of their much higher energy content,[18] C-protonated oximes were not taken into consideration. In general, **X/Y** stands for a transition structure (TS) connecting both equilibrium structures **X** and **Y**. Each structure is specified by a combination of a number and a letter: while the numbers are those mentioned above, the letters **Z**, **E**, and **D** stand for the *Z*-methyl, *E*-methyl, and dimethyl oxime, respectively. When the complex **4** is not considered, the TS **3/4** becomes thus **3/5**. To simplify the presentation of data, Figure 2 displays only selected MP2 geometrical parameters of the transition structures for the migration **3/4**. Some important changes in bond lengths and bond angles of the oxime skeleton upon methylation are recorded in Table 2.

Table 4. Zero-Point and Relative Energies of the *C*-Methyl Oxime Systems

structure		ZPE[a]	relative energy[b] MP4/6-311G(d,p)[c]
Z-$(H_3C)HC{=}N{-}OH$	**2Z**	220	−87
	3Z	213	0
	2/3Z	201	134
	4Z	203	−291
	3/4Z	195	15
	5Z	197	−174
E-$(H_3C)HC{=}N{-}OH$	**2E**	219	−77
	3E	213	0
	2/3E	200	137
	5E	199	−127
	3/5E	196	40
$(CH_3)_2C{=}N{-}OH$	**2D**	289	−90
	3D	283	0
	2/3D	270	123
	5D	271	−172
	3/5D	269	8
$H_2C{=}N{-}OCH_3$	**2M**	221	−60
	3M	217	0
	2/3M	202	150
	4M	201	−236
	3/4M	195	97
	5M	203	−58
$H_2C{=}N{-}OCH{=}O$	**2F**	173	−54
	3F	166	0
	2/3F	152	159
	4F	166	−305
	3/4F	149	63
	5F	160	−92

[a] Based on HF/6-31G(d) wavenumbers and scaled by 0.9. [b] Including MP4 relative energies and ZPEs. [c] Based on MP2/6-31G(d) geometries; core orbitals are frozen.

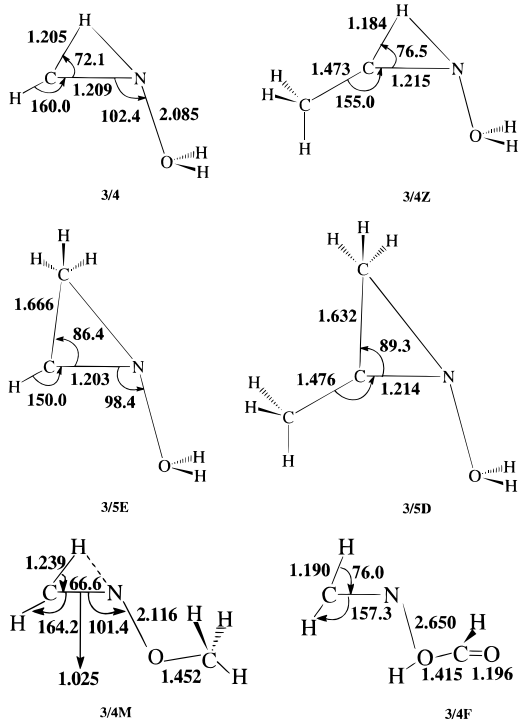

Figure 2. Selected geometrical parameters of the TSs for BR of substituted oximes at the MP2/6-31G(d) level. See text for definition.

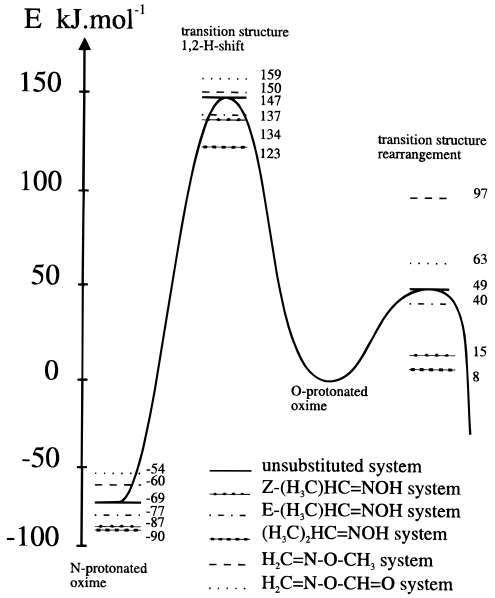

Figure 3. Schematic energy profiles showing 1,2-H-shift and BR of methylated derivatives. Values at the MP4/6-311G(d,p) // MP2/6-31G(d) +ZPE level.

Both C═N and N−O distances are marginally stretched upon methylation. The largest lengthening occurs in **3D** where the N−O distance increases to 1.605 Å. The CNO angles are not significantly affected either. Table 3 lists the calculated proton affinities (PA) of different oximes, while total, zero-point vibrational and relative energies of the relevant points are reported in Table 4. Results for oxime ethers (H_2C═N−OCH_3-(designated by **M**) and H_2C═N−O−CH═O (designated by **F**)) are also included but will be discussed in the following paragraph. At the level of theory employed, the PA of N of formaldehyde oxime (812 kJ·mol^{-1}) is apparently overestimated as compared with that of 799 kJ·mol^{-1} obtained from the MP4SDTQ/6-311++G(d,p) + ZPE results or that of 792 kJ·mol^{-1} from calculated heats of formation.[18] This quantity

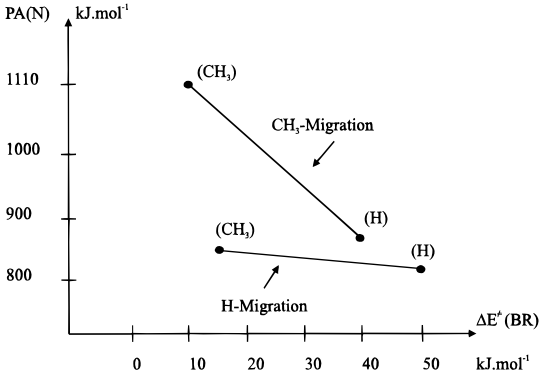

Figure 4. Crude correlation between energy barrier for BR and proton affinity at N of oximes. Nonmigrating groups are indicated in parentheses.

is uniformly increased following methylation. A geminal effect of two methyl groups attached to C enhances the basicity of both N and O centers, especially in favor of N. In monomethyl derivatives, both *Z*- and *E*-isomers have similar PAs at N, but the *Z*-isomer presents a larger gap between both PAs at N and O. The PA gap has the largest value in the dimethyl species. These observations can readily be rationalized by an additional stabilization of the carbocation **2a**:

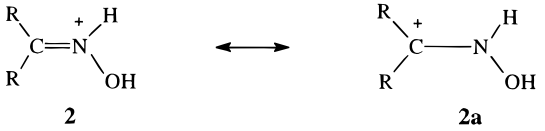

On the other hand, an unfavorable steric effect is likely to be responsible for a further destabilization of the O-protonated form **3Z**. As seen in Figure 3, stabilization of the N-protonated oxime **2**, relative to the O-protonated oxime **3**, upon methyl substitution consistently reduces the barrier height for the 1,2-H-shift from **3**, in line with the Hammond postulate. Inspection of Figure 3 and Table 4 indicates some essential phenomena with regards to the migration step from the O-protonated oxime **3**.

(1) Methyl is a slightly better migrating group than hydrogen. The energy barrier is lowered by 7−10 kJ·mol^{-1} when methyl migration is involved.

(2) The nonmigrating methyl group at C also exerts a positive effect by reducing quantitatively the energy barrier by 35 kJ·mol^{-1} in hydrogen migration and 32 kJ·mol^{-1} in methyl migration. Such energetic variations are not inconsistent with geometrical features of the TSs shown in Figure 2. The better migratory aptitude of methyl is manifested by an earlier TS: that is, on the one hand, the CCN angles in **3/5-E** and **3/5-D** are about 13−14° larger than the HCN angles in **3/4** and **3/4-Z**; on the other hand, the NO-bond breaking is somewhat more advanced in the former than in the latter (Figure 2). The relative migratory aptitude of both CH_3 and H groups is also related to the strengths of the C−C and C−H bonds; the average C−C bond energy is in fact smaller than the C−H bond energy (346 versus 411 kJ·mol^{-1}).[23]

In order to identify the character of the migrating group, a localization of molecular orbitals using the Boys' procedure[24] has been carried out. The spatial positions of the charge centroids of localized orbitals (LMO) allow the number and nature of bonding in any chemical entity to be specified and thereby the electronic reorganization to be determined. In the present case, LMO analysis suggests that in TS **3/4**, the

(23) Huheey, J. E. In *Inorganic Chemistry*; Harper Row: New York, 1972.

(24) Boys, S. F. *Rev. Mod. Phys.* **1960**, *32*, 296.

migrating group X moves with an electron pair of the C−X bond and thus behaves essentially as an anion X^- (X = H, CH_3). When the TS is passed, while this electron pair stays there forming the third bond of −C≡N−, X becoming now a cation is captured by the nitrogen lone pair to form a new N−X bond. Thus, before reaching the TS for migration, the carbon center becomes more positively charged, and such a structure is expected to be better stabilized by an electron donor methyl substituent than a hydrogen. As mentioned before, the migrating group X finally falls into the nitrogen lone pair; therefore, there exists a certain correlation between the barrier height and the nitrogen basicity as measured by PAs. Of course, the LMO analysis gives a picture of the HF wave functions which is not necessarily in line with that derived from higher level wave functions. Nevertheless in this case the energetic results obtained by HF and MPn calculations are internally consistent, suggesting that the HF-based LMO picture of the electronic distribution is realistic. For instance, using MP4 values, we have found that the larger the PA at N, the smaller the barrier height of the migration step is (Figure 4).

In summary, methyl substitution at carbon of oximes markedly accelerates the migration step. The energy barrier of 8 kJ·mol^{-1} for the dimethyl derivative is in fact too small to be real. It appears reasonable to assume that in C-dialkyl oximes, the migration is almost a barrier-free process. In contrast, the methyl effect on the 1,2-H-shift of N-protonated oxime is rather small, and the barrier remains quite high. In this context, the difficulty, if any, in converting an alkyl oxime to BR products resides in the formation of its O-protonated form, directly by protonation or indirectly from the more stable N-protonated form, rather than in the conversion of the O-protonated form.

(b) The Oxime Ether Species (H_2C=N−OR with R = CH_3, and HC=O). We now turn to the effect of substituents at oxygen. Methyl and formyl have been considered to model the electron-donor and electron-withdrawing groups. Relevant geometrical and energetic features have already been given in Tables 2 and 4 as well as in Figure 2. The simplest model species is in fact methyl oxime ether, H_2C=N−OCH_3 which is referred to by the letter **M**. A few important results emerge from calculations on this system.

(i) O-Methyl substitution also increases PAs but at a lesser extent than C-substitution (Table 3). The energy gap between both N- and O-protonated forms is reduced due to a stronger stabilization of the oxonium cation **3**.[25] As a consequence, the barrier height for the 1,2-H-shift of the latter, via TS **2/3M**, is enlarged, being thus the largest barrier among the four methylated systems.

(ii) The O-protonated species **3M** is also stabilized related to the product complex **4M** ($HCNH^+\cdots OHCH_3$) and the product fragments **5M**. This exerts a similar effect on the migration by putting the TS **3/4M** upwards on the energy scale. The barrier height turns out to be about twice as large as that of the unsubstituted species (Table 4). The geometry of TS **3/4M**, shown in Figure 2, consistently indicates a late transition structure having a smaller HCN bond angle.

The second substituent attached to oxygen that we have examined is the electron-acceptor formyl group, which is referred to by the letter **F**. It has been proposed[12] that when oxime is treated by a acetic acid solution (CH_3COOH/H^+), the reactive component of the BR is no longer the usual O-protonated oxime but actually an acetate ester (R_2C=N−O−$COCH_3$) or its protonated form (R_2C=N−OH^+−$COCH_3$). It is therefore important to find out whether there is any accelerating effect of the carbonyl group. The following results can be noted.

(i) Both PAs at N and O in formyl oxime ether are uniformly smaller than those of formaldehyde oxime. The PAs amount to 802 and 740 kJ·mol^{-1} in H_2C=N−O−$COCH_3$, as compared with 812 and 743 kJ·mol^{-1} in H_2C=N−OH, respectively.

(ii) The energies along the reaction pathways are (values in kJ·mol^{-1}) **2F** (−54) → **2/3F** (159) → **3F** (0) → **3/4F** (63) → **4F** (−305) → **5F** (-−2) as compared with the results obtained at the same level for unsubstituted species: **2** (−69) → **2/3** (147) → **3** (0) → **3/4** (49) → **4** (−260) → **5** (−121).

These similar minimum energy pathways suggest that, in gas phase, a carbonyl group does not create any genuine effect on the rate-controlling 1,2-H-shift. The difference in barrier heights between unsubstituted and O-formyl substituted species merely amounts to 3 kJ·mol^{-1}. Similar to the methyl substituted species, the formyl O-protonated form is overall stabilized relative to the N-protonated form, even though the electron withdrawing formyl group is expected to destabilize somewhat the oxonium cation. In contrast to the methyl case, the O-protonated form **3F** is destabilized relative to the product complex **4F** ($HCNH^+\cdots OHCOH$). This fact can be understood by the lack of resonance in **3F** which therefore could not compensate the destabilizing effect of the electron captor group on oxygen. As a result, an overall destabilization occurs.

It can thus be concluded that alkyl oxime ethers resist to the migration, whereas formyl oxime ethers do not affect this process at all. By way of extrapolation, any substituent at oxygen which could stabilize an oxonium cation (R_3O^+) is expected to slow down the process. Overall, our results indicate that the energy barrier of the rate-determining 1,2-H-shift is not modified significantly when substituent effects are taken into consideration.

Solvent Effects. Having established the rather small effect of substituents, we now turn to that of the solvent. We will successively examine both passive and active aspects of its influence on the BR.

(a) Electrostatic Influence. To evaluate the electrostatic influence of the solvent, we have first calculated the solvation energies using the classical self-consistent reaction field (SCRF)[20] model and the polarizable continuum model (PCM) developed by Tomasi and co-workers.[21] Overall, the solvation energy predicted by a simple SCRF model turns out to be negligible due to the fact that the dipole moment of the species involved are small. As a consequence, it is likely that these energies are not quite meaningful. In what follows, we only report the PCM results. In this model, the solvent cavity is directly reflected by the molecular shape, being constructed from atomic centered spheres of appropriate radii and the solvent polarization is modeled by virtual charges on the surface of the spheres. Within the latter model, we have also estimated the dispersion-repulsion and cavitation contributions to the solvatation energies of the various stationary points. The cavity term is the work needed to form the cavity where the solute must be accommodated. The dispersion-repulsion term is calculated with the procedure described in ref 27,[27] using the atom−atom potential parameters proposed by Caillet and Claverie.[28] The cavitation energy is expressed as a sum over the spheres forming the cavity

(25) Nguyen, M. T.; Hajnal, M. R.; Ha, T. K.; Vanquickenborne, L. G.; Wentrup, C. *J. Am. Chem. Soc.* **1992**, *114*, 4389.

(26) (a) Wong, M. W., Wiberg, K. B.; Frisch, M. J *J. Am. Chem. Soc.* **1992**, *114*, 523. (b) Wong, M. W., Wiberg, K. B.; Frisch, M. J. *J. Am. Chem. Soc.* **1992**, *114*, 1645. (c) Cieplak, A. S.; Wiberg, K. B. *J. Am. Chem. Soc.* **1992**, *114*, 9226.

(27) Floris, F. M.; Tomasi, J.; Pascual-Ahuir, J. L. *Compt. Chem.* **1991**, *12*, 784.

(28) Caillet, J.; Claverie, P. *Acta Crystallogr. B* **1978**, *34*, 3266.

$$G_{cav} = \sum_{i}^{spheres} \frac{A_i}{4\Pi R_i^2} G_i^{HS} \quad (4)$$

where R_i is the radius of the *I*th sphere and G_i^{HS} is the cavitation energy for a sphere of radius R_i in a fluid of hard spheres, according to Pierotti's expression.[29] A_i is the area of the portion of sphere *I* that is actually exposed to the solvent; the ratio $A_i/4\Pi R_i^2$ is a measure of the fraction of the sphere *I* that is not buried inside other spheres. The quantity $\sum_i^{spheres} A_i$ corresponds to the "van der Waals surface" defined by the surface of a cavity formed by the envelope of van der Waals spheres centered on atoms. An analysis of the relative weights of the different factors played in the solvation energy is summarized in Table 5. For the sake of simplicity, dispersion and cavitation terms are shown together. Both terms have only marginal influence on the final result as they nearly cancel out each other. While cavitation energies are always positive, dispersion contributions are negative, as expected from an interaction potential. The sum of both terms remains consistently small and almost constant from one structure to the other and thus induces only modest changes. As a consequence, the solvation energy can, in this case, be approximated solely by the electrostatic part. When the PCM treatment is used, a trend emerges, showing a small change in the rate-controlling barrier, namely about 10 kJ·mol^{-1}. Thus, a passive solvation of the medium does not allow us to recover the experimental results. As a polar medium increases the barrier height of the rate-determining step, there must be another way to facilitate it. The solvent is perhaps too often been regarded as a continuous medium, rather than an active participant in the reaction. In what follows, we intend to show that a direct participation of just one solvent molecule in the BR results in a fundamental modification of its course.

(b) Active Influence by Direct Participation. To model the active influence of a solvent, we used a supermolecule technique in which one solvent molecule is fully incorporated in the quantum mechanical calculations. This approach includes interactions that occur at relatively short distances in the vicinity of the solute. Three distinct media have been investigated. First, we examined the simplest solvent, namely water (H_2O), which is rather a hypothetical case but used here as a reference. Second, we examined the case of a "Beckmann mixture". This is one of the most employed solvents in practical use which is made of acetic acid and acetic anhydride, saturated with gaseous hydrogen chloride. HCl is obviously necessary for the protonation of the oxime. While the presence of the anhydride allows a low activity of water to be maintained in the solution; water being indeed formed upon dehydration of protonated oxime (see eq 1), the role of acetic acid is not clear. To probe its possible involvement in the BR, we have included an acid molecule in the supermolecule calculation. For computational reasons, formic acid (HCOOH) was investigated instead of CH_3COOH. Finally, we have also considered formaldehyde (H_2CO). This hypothetical solvent molecule has no hydroxyl group and allows one to probe further the effect of an acid functional group. Because the 1,2-H-shift connecting both N- and O-protonated oxime forms appears to be a key step of the entire BR process, as demonstrated in the proceeding paragraphs, we have only considered the effect of a solvent molecule on this step. Once the O-protonated species is formed, it is rapidly converted to the products either with or without the presence of solvent.

(29) Pierotti, R. A. *Chem. Rev.* **1976**, *76*, 717.
(30) Allen, M. P.; Tildesley, D. J. In *Computer Simulation of Liquids*; Clarendon Press: Oxford, 1987; Chapter 6.

Table 5. Dispersion, Repulsion, Cavitation, and Electrostatic Contributions to the Solvation Energies of the Considered Reaction Process in Water (in kJ·mol^{-1})[a]

	$\Delta G_{cav} + \Delta G_{dis}$	ΔG_{rep}	ΔG_{el}
N-protonated form	+13.2	+3.1	−289.5
TS 1,2-H-shift	+12.9	+3.1	−280.3
O-protonated form	+14.2	+3.1	−285.7

[a] The cavitation term is calculated using the model of Pierotti.[29]

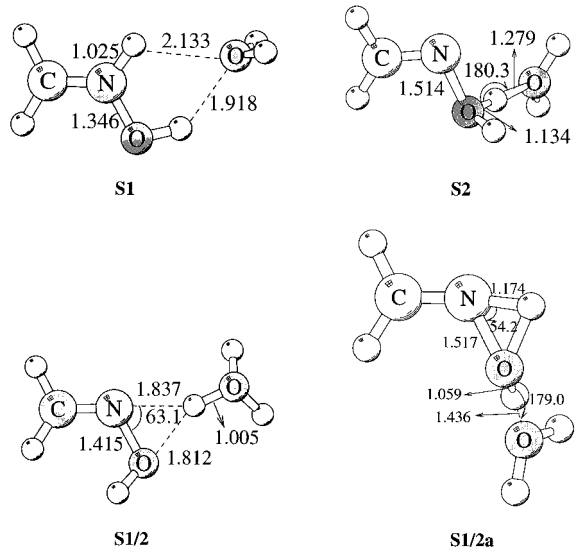

S1 **S2** **S1/2** **S1/2a**

Figure 5. Main geometrical features of the stationary points including the participation of a water (H_2O) molecule. Values at the MP2/6-31G-(d,p) level.

(A) Water as Solvent (H_2O). While the main geometrical features are shown in Figure 5, relative energies can be found in Table 6. The reaction starts with the N-protonated formaldoxime **2** and one separated H_2O molecule. The water molecule can form hydrogen-bonded complexes with both protonated oximes. At the MP4SDTQ/6-311++G(d,p)//MP2/6-31G(d,p) + ZPE level, the complexation energy amounts to −92 and −114 kJ·mol^{-1} for the N-protonated and O-protonated forms **S1** and **S2**, respectively. In **S1**, only weak interactions occur between the water oxygen and both hydrogens of the N-protonated oxime (2.133 and 1.918 Å, respectively). Both water hydrogens are turned away from the oxime. This orientation allows a good electrostatic interaction between both oxime and solvent molecules and turns out to be the most stable of all possible configurations. The complex **S2** results mainly from a OH···O interaction with a shorter intermolecular distance. The connection between both complexes **S1** and **S2** proceeds via transition structure **S1/2**. The activation energy is calculated to be 97 kJ·mol^{-1}, relative to **S1**, which is actually 128 kJ·mol^{-1} lower than the gas phase reaction (225 → 97 kJ·mol^{-1}) and approximates the experimental values obtained in different media.[15−16] Table 6 indicates that this barrier height is sensitive to the basis set size and the inclusion of electron correlation.

Beyond the nonplanarity of the hydroxyl hydrogen, we have found that, in TS **S1/2**, the migrating hydrogen is almost fully transferred from oxime to water. The NH···OH_2 distance changes in fact from 2.133 Å in **S1** to 1.005 Å in TS **S1/2**. The solvent molecule exerts its influence by preassociating the N-protonated oxime through a complex **S1** and facilitating the hydrogen migration yielding an O-protonated oxime···H_2O(+) complex **S2**, by means of an hydrogen transfer. Apparently, the TS **S1/2** looks like a complex between a formaldoxime molecule and a H_3O^+ cation. Nevertheless, analysis of the normal coordinates of the imaginary vibrational mode points out that it corresponds well to a transition structure linking both

Table 6. Zero-Point and Relative Energies[a] of the BR Stationary Points Including a H_2O Molecule

	ZPE[b]	MP2 6-31G(d,p)[c]	MP2 6-311G(d,p)[d]	MP4SDTQ 6-311G(d,p)[e]	MP4SDTQ 6-311++G(d,p)[e]
2 + H_2O	204	−83	−82	−75	−77
S1	213	−192	−185	−182	−169
S1/2	206	−97	−93	−86	−72
S1/2a	193	28	36	41	53
S2	205	−136	−130	−127	−114
3 + H_2O	198	0	0	0	0

[a] Including ZPE corrections. [b] Obtained from HF/6-31G(d,p) vibrational wavenumbers, scaled with 0.9. [c] Using full sets MOs. [d] Based on HF/6-31G(d,p) geometries. [e] Based on MP2/6-31G(d,p) geometries.

complexes **S1** and **S2**. The connection is further confirmed by intrinsic reaction coordinate (IRC) calculations. As shown in Figure 8, such a direct interaction induces an extra stabilization of the transition structure and therefore accelerates the 1,2-H-shift considerably. An alternative transition structure (**S1/2a**) in which the interaction of a H_2O molecule occurs on the a nonmigrating hydrogen has only a slight influence on the barrier height (Figure 5 and Table 6). In going from gas phase to H_2O solution, only a tiny reduction of the energy barrier of the 1,2-H-shift (225 → 222 kJ·mol^{-1}) occurred through TS **S1/2a**. Absence of an extra stabilization by hydrogen transfer does not create any accelerating influence. It is thus clear that a positive effect is only found for a direct interaction between, at least, one solvent molecule and the transferring hydrogen. From both geometrical and energetic points of view, the action of the water molecule can be regarded as that of a catalyst.

At this stage, a question of interest is whether such a catalytic effect of H_2O might be more efficient through a cyclic mechanism. In this hypothesis, water molecules behave bifunctionally in cyclic structures as proton donor and proton acceptor. The corresponding reaction coordinate might be dominated by simultaneous proton transfers coupled with the making and breaking of the O−H and N−H bonds. Such a TS (see **TS1**) is expected to involve a nucleophic attack of a H_2O oxygen on the hydrogen of N-protonated oxime followed by a concerted transfer of a H_2O hydrogen to the oxime oxygen to form the O-protonated isomer.

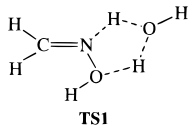

TS1

However, in spite of intensive search, we were not able to locate the related cyclic minimum and transition structure **TS1**. Geometry optimizations repeatedly converged to the already known structures, namely both minima **S1**, **S2**, and TS **S1/2**. These results suggest that the H_2O molecule exerts its active role in the rate-determining 1,2-H-shift not via a bifunctional acid−base cyclic process but rather via a hydrogen transfer.

In considering the advantages and limitations of the microscopic and continuum models, it seems natural to consider a mixed scheme to simulate the solvent effect. In such an approach, a first solvation shell is built up by considering a finite number of solvent molecules, and then the remaining part is treated according to the continuum model.[22] The solute molecule is treated quantum mechanically and is called the *quantum system*. In the next step, the first solvation layer around the solute is taken into account explicitly using a classical model. A number of subsystems may be defined and are treated in a discrete classical way. The vacuum static potential of these subsystems is reproduced by an expanded monopole representation. The response potential is for its part mediated through anisotropic dipole polarizabilities (usually one per subsystem). The quantum plus discrete classical systems may be enveloped by a surface that defines the boundary between both discrete and continuum parts. The latter, situated outside the boundary, can be classically modeled by a single response parameter, namely the dielectric constant ϵ, which describes the collective response of a large number of molecules to an applied electric field. We used the formalism developed by Van Duijnen and co-workers[22] whose essential features have been implemented into the HONDO8 program and renamed HONDRF. Concretely, in this case, 26 classical solvent molecules surround the protonated oxime plus H_2O system (**S1**, **S2**, and TS **S1/2**). The solute and solvent molecules are in turn surrounded by a dielectric. In addition a modest Monte Carlo (MC) sampling[30] of the translational and orientational degrees of freedom of solvent molecules was performed. The number of MC steps was limited to 10 000 because of extremely high CPU time demands. Results obtained show that MC sampling does not change the qualitative picture given above but instead modifies slightly the quantitative aspect.

At the HF/DZP//MP2/6-31G(d,p) level, the activation energy for the 1,2-H-shift catalyzed by a H_2O molecule is calculated to be 89 kJ·mol^{-1} with the continuum effect, which is 33 kJ·mol^{-1} lower than the value without the latter. Such a difference can be attributed to an explicit consideration of hydrogen bonding interactions in the MC calculations which is obviously important for simulation in water. For the sake of completeness, we also considered the combined solvent model on the gas phase reaction path of protonated formaldehyde oxime whithout any active help of solvent molecules. In the latter case, barrier heights are also found to be reduced through a modest MC sampling of the solvent degrees of freedom. For the 1,2-H-shift, the reduction of the activation energy amounts to 21 kJ·mol^{-1}, whereas the barrier to rearrangement is lowered by 25 kJ·mol^{-1}. Such small variations lend further support for the results discussed above concerning the importance of an active solvent participation.

(B) Formic Acid as Solvent (HCOOH). Optimized geometrical parameters of the catalytic reaction path are given in Figure 6. Figure 9 shows the energy profiles determined at the MP2/6-311G(d,p) + ZPE level based on HF/6-31G(d,p) geometry for both the uncatalyzed gas phase reaction path as well as that of the catalyzed reaction path involving direct participation of one formic acid molecule. Selected relevant total and relative energies are reported in Table 7. There exists a quite stable five-membered ring complex **S3** made up from the N-protonated oxime **2** and formic acid which lies about 93 kJ·mol^{-1} below the corresponding separated system. The N−H···OCHOH distance is fairly long being 2.013 Å, and the complex **S3** has C_s symmetry. The complex **S4** involving the O-protonated oxime and formic acid results from a O−H···O interaction, and the associated complexation energy is also large (100 kJ·mol^{-1}). It appears again that these complexes play an essential role in the catalytic process resulting in a "preassociation mechanism" where reactants are oriented configurationally in an optimal

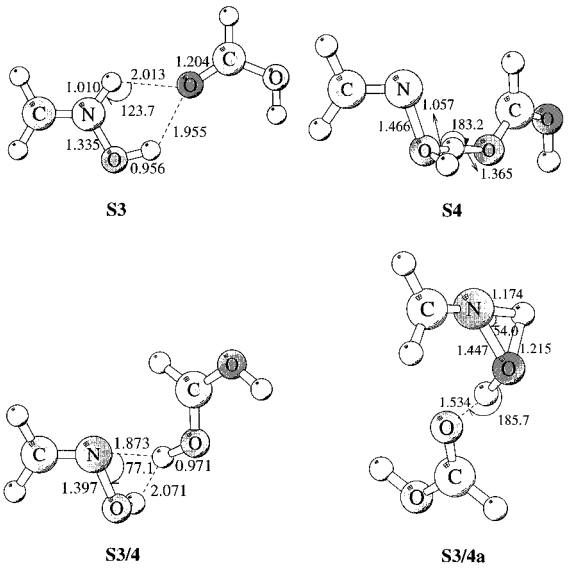

Figure 6. Main geometrical features of the stationary points including the participation of a formic acid (HCOOH) molecule. Values at the MP2/6-31G(d,p) level.

Table 7. Zero-Point and Relative Energies[a] of the Critical Stationary Points Including an Active Formic Acid Molecule (HCOOH)

		ZPE[b]	MP2/6-311G(d,p)[c]
$H_2C{=}NH{-}OH(+) + HCOOH$		237	−81
$H_2C{=}NH{-}OH\cdots HCOOH(+)$	**S3**	242	−181
TS (1,2-hydrogen-shift) (+)	**S3/4**	237	−102
TS (1,2-hydrogen-shift) (+)	**S3/4a**	206	+40
$H_2C{=}N{-}OH_2\cdots HCOOH(+)$	**S4**	233	−129
$H_2C{=}N{-}OH_2(+) + HCOOH$		231	0

[a] Including MP2 relative energies and ZPEs. [b] Based on HF/6-31G(d,p) wavenumbers and scaled by 0.9. [c] Based on HF/6-31G(d,p) geometries.

fashion to permit an accelerated 1,2-H-shift. The geometry of TS **S3/4** is nonplanar, and the distances between the migrating hydrogen and N and O of the oxime are 1.873 and 2.071 Å, respectively (Figure 6). As in the H_2O case, one solvent molecule catches the migrating hydrogen at the TS and puts it on the oxime oxygen yielding the O-protonated oxime···HCOOH (+) complex **S4**. Such a direct action of one formic acid molecule is clearly beneficial and reduces the energy barrier dramatically, relative to the gas phase (228 → 79 kJ·mol^{-1}). This implies a considerable acceleration of the most energy demanding step of the Beckmann transformation (Figure 9). The transition structure in which a specific interaction between a formic acid molecule and the migrating hydrogen is omitted has also been located, namely the TS **S3/4a** (Figure 6). In this case the solvent reduces the barrier height by only 23 kJ·mol^{-1} relative to the gas phase value (228 → 205 kJ·mol^{-1}). Another possibility in which the reaction would be proceeded via a bifunctional cyclic TS does not exist; similar to the H_2O case, our extensive calculations do not lead to the proposed structures. To probe the nonspecific influences of the continuum, SCRF calculations were also carried out. The results suggest that electrostatic interactions do not initiate a significant modification of the energy surface, but even cause a slight increase of the activation energy (79 →8 5 kJ·mol^{-1}). This is presumably due to the differences in dipole moments. In view of the small changes, we have not pursued further PCM or Monte-Carlo calculations on this system.

(C) Formaldehyde as Solvent ($H_2C{=}O$). The last part of our investigation is to check whether an acid function is really needed to catalyze the 1,2-H-shift. To resolve this question, we have considered formaldehyde ($H_2C{=}O$) as solvent and calculated the reaction paths analogous to those involving water (H_2O) and formic acid (HCOOH). As formaldehyde has no OH group, the results allow the catalytic power of both functional groups to be compared. Selected total energies and relative energies of the calculated reaction paths are reported in Table 8. Geometrical features are given in Figure 7, while Figure 10 compares the barrier heights for both uncatalyzed and catalyzed cases. Similar to water and formic acid, a catalytic effect only occurs by strong interaction between a $H_2C{=}O$ molecule and the migrating hydrogen which again is fully transferred (see TS **S5/6**). Stabilization energies are rather sensitive to electron correlation. In fact, the complexation energy between formaldehyde and the N-protonated oxime giving **S5** is computed to be −93 kJ·mol^{-1} at HF/6-31G(d,p) but −107 kJ·mol^{-1} at MP4/6-31G(d,p). However, results derived from MP2, MP4SDTQ, and QCISDT calculations with the 6-31G(d,p) basis sets are comparable to each other which amounts to −99 kJ·mol^{-1} at the QCISDT/6-31G(d,p)//MP2/6-31G(d,p) + ZPE level. The corresponding value for complex **S6** is about −113 kJ·mol^{-1}. Introduction of $H_2C{=}O$, acting as a proton-relay catalyst, reduces the energy barrier by about 125 kJ·mol^{-1} (225 → 100 kJ·mol^{-1}). Thus, the barrier height in this case is larger than those in water and formic acid, 97 and 79 kJ·mol^{-1}, respectively. This difference can be attributed to a variation in proton affinities (PA) of the solvents under consideration. Calculated proton affinities (727 kJ·mol^{-1} for HCOOH and 712 kJ·mol^{-1} for $H_2C{=}O$ at the same level) indicate a certain correlation between the solvent molecule PA and the energy barrier to 1,2-H-shift. The larger the PA, the stronger the tendency of the solvent to catch a proton. Such behavior results in a longer bond length between the oxime and the migrating hydrogen, as clearly seen in the corresponding transition structures (Figure 7). Distances between formaldehyde and both N and O of the oxime are 1.848 and 2.010 Å, respectively. In the case of formic acid these bond lengths are somewhat lengthened (1.873 and 2.071 Å, respectively). Hence, the stronger the stabilizing interaction between the migrating hydrogen and the solvent in the transition structure, the lower the energy barrier to 1,2-H-shift. It thus emerges that a solvent having the larger proton affinity (PA) induces a more positive catalytic effect. This is in line with the experimental fact mentioned in the Introduction, namely solvents of high nucleophilic power tend to increase the rearrangement rate. Similar to the results for water and formic acid, TS **5/6a**, involving any specific interaction, shows no remarkable catalytic effect. We even note a slight increase of the energy barrier to 1,2-H-shift (225 → 227 kJ·mol^{-1}). These results suggest that, from an electronic viewpoint, there is only a marginal difference between $H_2C{=}O$ and HCOOH as solvent molecules.

In order to evaluate the entropy effects, we have also calculated total and relative entropies of the stationary points in both formaldehyde and formic acid cases. Starting from the N-protonated oxime-solvent complex, the entropy variation amounts to about 130−140 J·mol^{-1}·K^{-1}. The corresponding entropy contribution $T{\cdot}\Delta S^{\ddagger}$ is found to be small for both solvents and amounts to about 4 kJ·mol^{-1} for formic acid and 3 kJ·mol^{-1} for formaldehyde. These values lie well below the expected errors for ab initio MO calculations at the levels considered here. In view of the results concerning both geometrical and energetic aspects of the catalytic action, it seems reasonable to admit that an intervention of a second solvent molecule in the reaction process is no longer a crucial factor.

Table 8. Zero-Point and Relative Energies[a] of the Stationary Points Including a H_2CO Molecule

	ZPE[b]	MP2 6-31G(d,p)[c]	MP2 6-311G(d,p)[d]	MP4SDTQ 6-31G(d,p)[e]	QCISD(T) 6-31G(d,p)[e]
2 + H_2CO	217	−83	−81	−74	−74
S5	224	−183	−178	−174	−173
S5/6	221	−81	−77	−73	−73
S5/6a	204	38	67	49	54
S6	217	−122	−114	−115	−113
3 + H_2CO	211	0	0	0	0

[a] Including ZPEs. [b] Obtained from HF/6-31G(d,p) vibrational wavenumbers, scaled with 0.9. [c] Using full sets MOs. [d] Based on HF/6-31G(d,p) geometries. [e] Based on MP2/6-31G(d,p) geometries.

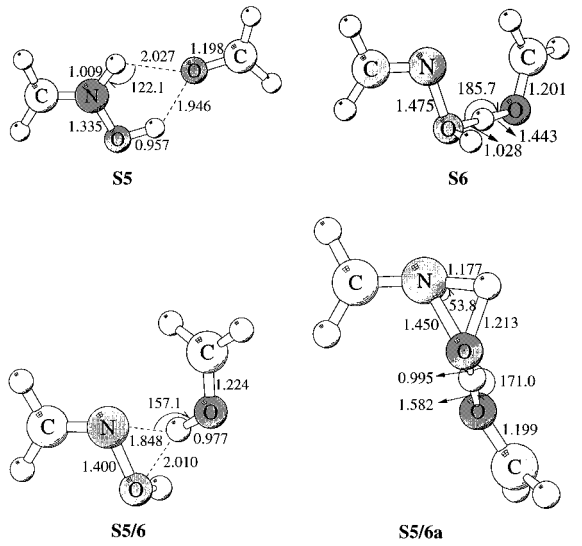

Figure 7. Main geometrical features of the stationary points including the participation of a formaldehyde (H_2CO) molecule. Values at the MP2/6-31G(d,p) level.

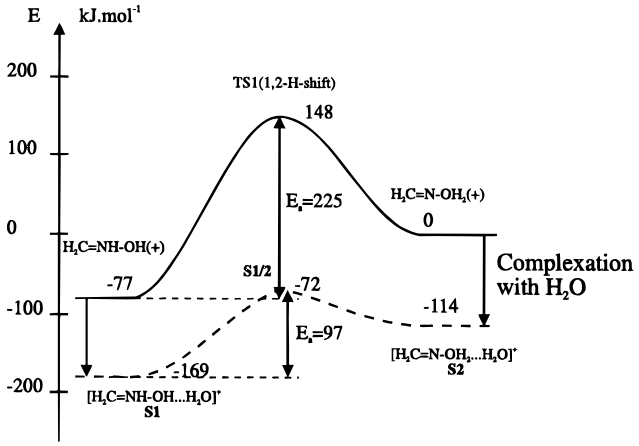

Figure 8. Schematic energy profile of the rate-controlling 1,2-H-shift for both processes in gas phase and catalyzed by a specific interaction between a water molecule and the migrating hydrogen. Values at MP4/6-311++G(d,p) + ZPE level, based on MP2/6-31G(d,p) geometry.

Summary

In this paper we have examined both substituent and solvent effects on the Beckmann process. The migration-fragmentation of an O-protonated oxime is much easier to realize than the conversion to its N-protonated isomer. Proceeding from the N-protonated oxime, which is the most stable form and thus the most populated isomer upon protonation, the rate-determining step is consistently the 1,2-hydrogen migration connecting both protonated forms. Methyl substitution at carbon strongly influences the fragmentation by reducing its energy barrier. The dimethyl derivative has a calculated barrier of about 8 kJ·mol^{-1}. Therefore, the BR of alkyl oximes is expected to be mainly

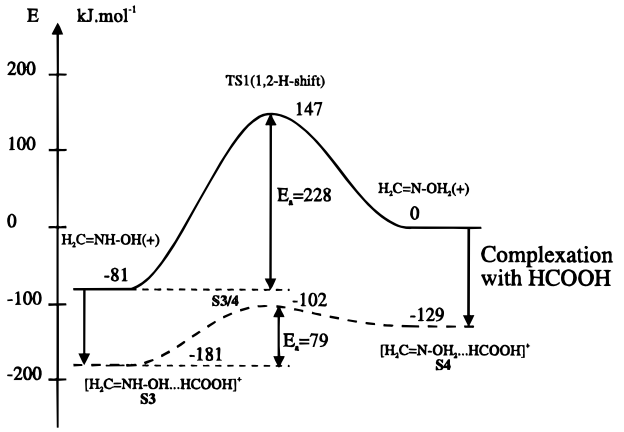

Figure 9. Schematic energy profile of the rate-controlling 1,2-H-shift for both processes in gas phase and catalyzed by a specific interaction between a formic acid molecule and the migrating hydrogen. Values at MP2/6-311G(d,p) + ZPE level, based on HF/6-31G(d,p) geometry.

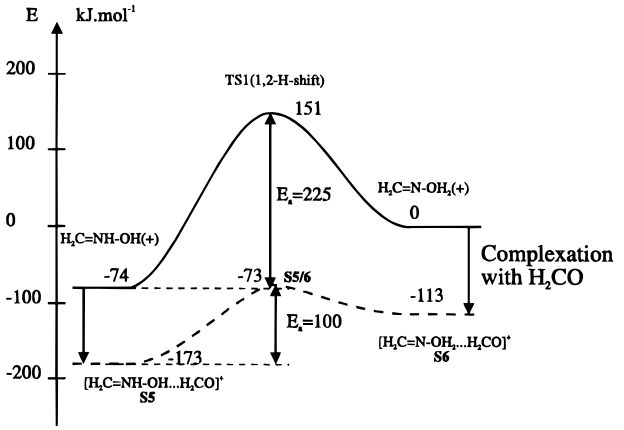

Figure 10. Schematic energy profile of the rate-controlling 1,2-H-shift for both processes in gas phase and catalyzed by a specific interaction between a formaldehyde molecule and the migrating hydrogen. Values at QCISDT/6-31G(d,p) + ZPE level, based on MP2/6-31G(d,p) geometry.

conditioned by the formation of their O-protonated species. Both methyl and formyl substitution at oxygen slows down the fragmentation while they do not induce a significant effect on the barrier height to 1,2-H-shift. Calculations, modeling the solvent effects, using the PCM continuum model and a combination of both quantum and statistical mechanical treatments, predict that the resulting activation energy of the rate-controlling 1,2-H-shift is not modified significantly with respect to the corresponding one obtained in gas phase. In contrast, an active participation of one solvent molecule in the reacting supersystem gives rise to a genuine effect. In general, there exists a quite strong five-membered ring complex made from N-protonated oxime and a solvent molecule. It appears that this complex plays an important role permitting a preassociation mechanism where the reactants are oriented in an optimal

manner creating the most favorable spatial conditions for a proton transfer in a rapid and subsequent step. Calculations using a direct reaction field approach also emphasize rather small modifications on energetic parameters from the bulk solvent system. Our results consistently suggest that the BR constitutes a strong case of active solvent catalysis where the solvent molecules take place as a homogenous catalyst in the chemical process. The catalytic effect results in an interaction between the migrating hydrogen and a solvent molecule which in turn favors the migration by a transfer of the hydrogen to the solvent molecule at the transition state. The calculated energy barriers with an active participation of a solvent molecule approximate more closely the experimental results in solution. A crude correlation between solvent proton affinities and barrier heights can be established; the larger the solvent PA, the faster the hydrogen transfer and the stronger the catalytic effect induced by the solvent.

Acknowledgment. We wish to thank the Flemish Science Foundations (FWO, IWT, and GOA), and the KU Leuven Computing Centre for continuing support. We are also grateful to Betty Coussens, Jacopo Tomasi, and Piet Van Duijnen for helpful discussion.

Supporting Information Available: Tables 4a, 6a, 7a, and 8a contain the total energies (in hartrees) related to relative energies given in Tables 4, 6, 7, and 8 (2 pages). See any current masthead page for ordering or Internet access instructions.

JA962364Q